On the destruction of the hidden order in URu_2Si_2 by a strong magnetic field

Julien Levallois[1], Kamran Behnia[2], Jacques Flouquet[3], Pascal Lejay[4] and Cyril Proust[1]

[1] *Laboratoire National des Champs Magnétiques Pulsés (UMR 5147 CNRS-UPS-INSA), Toulouse, France*
[2] *Laboratoire Photons et Matière (UPR5-CNRS), ESPCI, 10 Rue de Vauquelin, 75231 Paris, France*
[2] *Institut Nanosciences et Cryogénie, SPSMS/MDN, CEA-Grenoble, 38054 Grenoble, France*
[2] *Institut Néel, CNRS/UJF, B.P. 166, 38 042 Grenoble Cedex 9, France*

arXiv:0809.4715v2 [cond-mat.str-el] 30 Apr 2009

PACS 71.27.+a – Strongly correlated electron systems; heavy fermions
PACS 72.15.Gd – Galvanomagnetic and other magnetotransport effects
PACS 75.30.Mb – Valence fluctuation, Kondo lattice, and heavy-fermion phenomena

Abstract. - We present a study of transport properties of the heavy fermion URu_2Si_2 in pulsed magnetic field. The large Nernst response of the hidden order state is found to be suppressed when the magnetic field exceeds 35 T. The combination of resistivity, Hall and Nernst data outlines the reconstruction of the Fermi surface in the temperature-field phase diagram. The zero-field ground state is a compensated heavy-electron semi-metal, which is destroyed by magnetic field through a cascade of field-induced transitions. Above 40 T, URu_2Si_2 appears to be a polarized heavy fermions metal with a large density of carriers whose effective mass rapidly decreases with increasing magnetic polarization.

INTRODUCTION. – Discovered more than twenty years ago [1–3], the order which emerges in URu_2Si_2 below T_0=17.5 K remains as enigmatic as ever. This unidentified order parameter (proposed to be associated with orbital degrees of freedom [4,5], a spin density wave [6,7], orbital magnetism [8] or magnetic helicity [9]) is commonly called the hidden order (HO) state. For a long time, it was associated with a tiny ordered moment ($M_0 \sim 0.02\mu_B$ per U atom) [10], which did not match the large anomalies detected in the macroscopic properties at T_0. A consensus on the extrinsic nature of this tiny moment is gradually emerging, since its size decreases with improvement in sample quality [11]. On the other hand, a true antiferromagnetic (AF) ground state with a large ordered moment (0.3 μ_B/U) and an identical wave vector (0,0,1) emerges above a rather small critical pressure P_x of 0.5 GPa [11,12]. The first order HO-AF boundary meets the HO and AF lines at a tricritical point at $P_c = 1.2$ GPa. The tiny moment at zero pressure appears to be a consequence of the difficulty to obtain samples in which local stress is totally removed [11,13].

The study of transport properties has established a radical reconstruction of the Fermi surface below T_0. An early study of the Hall effect (using a simplified one-band model) had already concluded that the carrier density in the hidden-order state is as low as 0.03 carriers per formula unit (f.u.) [14] implying that the carrier density is more than one order of magnitude lower than in the unordered state and what is predicted by band calculations. A large drop in carrier density in the HO state provides a natural explanation for a drastic enhancement of phonon thermal conductivity [15, 16]. Moreover, the carrier concentration deduced from the Hall data is compatible with the largest of the small frequencies detected in the de Haas- van Alphen (dHvA) and Shubnikov-de Haas (SdH) measurements [17–19] and the large magnetoresistance observed in the new generation of ultraclean crystals [20]. Thus, the state which emerges below T_0 is a dilute liquid of heavy quasi-particles, with Fermi surfaces occupying a fraction of the Brillouin zone much smaller than what it is expected according to band calculations. Such a context indicates a Fermi surface reconstruction based either on a nesting scenario associated with a density wave instability [21] or on a change in the lattice symmetry.

However, several puzzles face any scenario based on nesting. The first problem is to identify a plausible nesting vector. In neutron scattering measurements in the hidden order phase, except the extrinsic tiny antiferromagnetic moment at Q_{AF}=(0,0,1), two main inelastic magnetic responses of Q_0=(1,0,0) and Q_1=(0.4,0,1) have been

detected. One suggested candidate is the incommensurate wave vector Q_1=(0.4,0,1) for a spin density at T_0 [21]. Under pressure above $P_x \simeq$0.5 GPa in the AF phase at low temperatures, the inelastic response at Q_0 has disappeared while the excitations at Q_1 persists and has shifted to a higher energy than at $P = 0$ [13]. However, a nesting wave vector along either Q_1 or Q_0 is not obvious from the point of view of band calculations in the paramagnetic regime [22]. The second problem comes from the behavior of transport and thermodynamic properties under pressure. While a phase transition clearly occurs between the hidden ordered state (stabilized below T_0 for pressures below P_c) and the AF phase (stabilized below T_N for pressures above P_c) [23], resistivity and specific heat anomalies remain unaltered across P_c [12]. This indicates that the ordering leads to a radical reconstruction of the Fermi surface both below and above P_c. In other words, if there is nesting, it seems to be indifferent to presence or absence of the large AF ordered moment. Recent inelastic neutron diffraction experiments under pressure lead to propose that the same wave vector Q_0 characterize the hidden order and the AF phases [13]. At T_0 or T_N, the crystal structure changes from body centered tetragonal to tetragonal, implying a carrier density drop by a factor between 3 and 5, according to recent band structure calculations [22, 24].

The hidden order is destroyed by the application of a strong magnetic field [25]. Interestingly, the application of magnetic field, which weakens the partial Fermi surface gap [26], leads to an enhancement of the gap magnetic excitations at Q_0, while the one at Q_1 slowly decreases [27]. Studies of transport [28–31] and thermodynamic properties [32, 33] have shown that a cascade of phase transitions occurs at low temperature when magnetic field ranging from 35 T to 39 T is applied parallel to the easy c-axis, leading to the destruction of the hidden order. Above 39 T, a polarized paramagnetic (PPM) metal is restored via successive jumps of magnetization near 0.3 μ_B [25, 34–36]. Thus, the metamagnetic transition, a recurrent feature of heavy fermion physics, takes a particularly complicated twist in presence of the hidden order.

In this paper, we report on a study of transverse magnetoresistance (MR) and Hall effect in URu_2Si_2 in pulsed magnetic field up to 55 T. We also present the first measurements of the Nernst effect in pulsed magnetic fields in the hidden order phase. According to our results, the large Nernst response which emerges below T_0 [38] is suppressed above 35 T. Hence, it is a property of the hidden-order state. Moreover, and in agreement with previous studies, we find that the hidden order and the high-field PPM state are separated by two other unidentified ground states. Thus, three successive field-induced Fermi surface reconstructions occur before the stabilization of the polarized high-field state. The latter happens to be a metal with a high density of carrier, in sharp contrast with the zero-field one: It has a large Fermi surface and low electronic mobility.

Experimental. – Single crystals of URu_2Si_2 were prepared in a three-arc furnace under a purified argon atmosphere and annealed under UHV for one week at 1050 °C. Different samples with typical residual resistivity $\rho_0 \approx 7\ \mu\Omega cm$ and typical dimensions (2×1×0.03) mm^3, have been measured. In the four-probe resistivity measurements, the current was injected along the a-axis of the crystals and magnetic fields was applied along c-axis. The resistivity of each sample was measured at a given fixed temperature during the magnetic field pulse using a lock-in amplifier working at 50 kHz.

A special set-up to measure the Nernst effect in presence of a pulsed field was designed. Its technical details will be published elsewhere [39]. The transverse Nernst voltage produced by a DC thermal gradient, $\Delta T \approx 1\ K$ along the sample was measured with a low-noise pre-amplifier. The thermal gradient and the temperature of the sample were measured with two Chromel/Constantan thermocouples before and after pulsing the magnetic field. The field dependence of the thermal gradient (as expected from the field dependence of thermal conductivity [15]) was neglected. In the temperature range of investigation, heat conduction is dominated by the phonon contribution. The available data up to 12T [15] suggest that at T=3 K, the field-induced change in thermal gradient could modify the magnitude of the Nernst signal by 50 percent. This would not alter any of our conclusions. In order to get the required signal/noise ratio, in particular to reduce mechanical vibrations, we have used a magnet whose maximum field is 36 T.

Cascade of phase transitions. – Fig. 1(a) shows the field dependence of the transverse magnetoresistance ($\mathbf{I} \parallel \mathbf{a}$ and $\mathbf{B} \parallel \mathbf{c}$), above and below the hidden order transition temperature T_0=17.5 K.

As originally reported by Bakker and co-workers [28], three field distinct field scales can be identified between 35 T and 40 T. During the past few years, high-field studies of specific heat [32], ultrasound [40] magnetization [33], resistivity [29, 31] and Hall effect [30] have identified several phases (up to five) in this field window. The three field scales identified in our low field data allows to distinguish between four states, which, following previous authors, are labelled from I to IV.

Phase I ($B < 35\ T$). The zero-field ground state (i.e., the hidden order state) remains the ground state up to $B_{HO} = 35\ T$. One of its remarkable properties is a large Hall number ($R_H = \rho_{xy}/B$). Our data yields $R_H \sim 10^{-8} m^3/C$ at T=2 K. This magnitude is close to the value reported in crystals of comparable residual resistivity [28, 30, 38]. In a simple one-band picture, it would yield to an effective carrier density of $n_H = 1/eR_H \approx$0.05 carrier per U atom.

Band structure calculations [19, 22, 24] categorize URu_2Si_2 as a compensated metal. The fact that the mag-

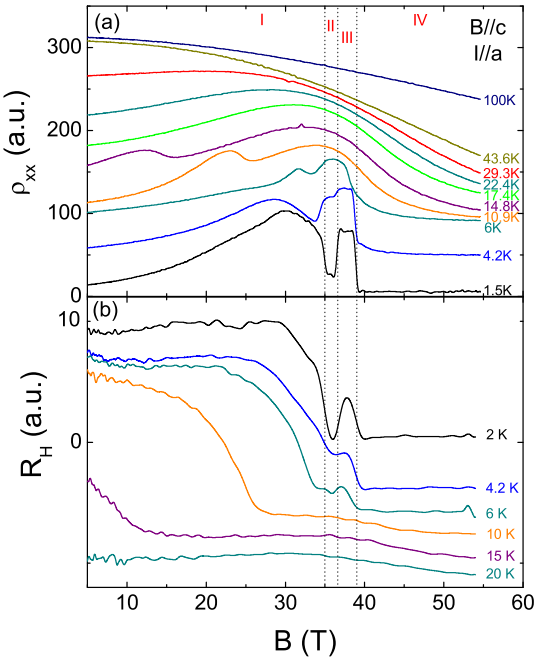

Fig. 1: (a) Magnetic field dependence of the transverse magnetoresistance in URu_2Si_2 at different temperatures. The labels on the left axis stand for the curve at T=1.5 K in $\mu\Omega cm$. The other curves are shifted for clarity. The labels I-IV denote the different parts of the phase diagram [29] (b) Magnetic field dependence of the Hall coefficient in URu_2Si_2 at different temperatures. The labels on the left axis stand for the curve at T=2 K in $10^{-3}cm^3/C$. The other curves are shifted for clarity.

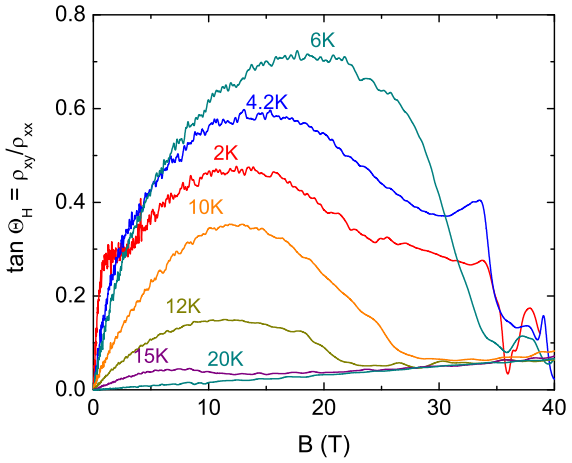

Fig. 2: Magnetic field dependence of the Hall angle of URu_2Si_2 at different temperatures

netoresistance does not saturate in the hidden order up to 20 T in ultraclean crystals where $\omega_c\tau >> 1$ [20] indicates that URu_2Si_2 is a compensated semi-metal.

Fig. 2 shows the magnetic field dependence of the Hall angle defined as $\tan\Theta_H = \rho_{xy}/\rho_{xx}$. The entrance in the hidden order state is concomitant with the appearance of a large Hall angle. In a simple one-band picture the Hall angle is a measure of $\omega_c\tau = \mu B$, where $\mu = e\tau/m^*$ is the mobility. Its large magnitude in the hidden order state is a consequence of the enhanced carrier mobility.

In the hidden order state, the magnetoresistance is quadratic up to ≈20 T(see fig. 3). In a simple one-band picture, the magnitude of the magnetoresistance is intimately related to mobility μ via the relation $\frac{\Delta\rho(B)}{\rho_0} \propto (\omega_c\tau)^2 = (\mu B)^2$. In our case, a field of 20 T leads to a 4-fold increase in resistivity. It is instructive to compare the slope of $\frac{\Delta\rho(B)}{\rho_0}$ as a linear function of B^2 with the one reported for an ultraclean crystal [20]. The large difference (it was 3 T^{-2} there compared to 0.011 T^{-2} here) implies a mobility ratio equal to 16.5, in good agreement with the 14-fold difference in the magnitude of residual resistivities (7 $\mu\Omega$cm here and 0.5 $\mu\Omega$cm there). This is a good check of the overall consistency of this analysis. This is further confirmed by the validity of the Kohler's rule in the hidden order state (see inset of fig. 3) and by the value of the mobility deduced from magnetoresistance, $\mu \approx 0.1$ T^{-1}, in good agreement with the low-field slope of $\tan\Theta_H(B)$.

The combination of a small Fermi surface and high mobility suffice to explain the large Nernst signal, which emerges in the hidden-order state. [38] The Nernst coefficient is defined as $N = E_y/\nabla_x T$, where E_y is the electric field generated by the combined application of a longitudinal thermal gradient and a transverse magnetic field.

In order to check that the large Nernst signal is a property of the hidden order state, we have performed the first study of the Nernst effect in pulsed magnetic fields up to 36 T. Fig. 4 shows the field dependence of the Nernst signal at different temperatures in the hidden order state. The magnitude of the Nernst signal found here is twice lower than the data reported for B <12 T [38]. The discrepancy may be a consequence of the uncertainty on the magnitude of thermal gradient. At low temperature and for magnetic field up to ∼20 T, the Nernst signal varies linearly with field and reaches a maximum of $N \simeq 30$ μV/K at T=3 K. Taking the sign change of the Nernst signal changes as the signature of the destruction of the hidden order state, we obtain the phase diagram (B, T) shown in the inset of Fig. 4, which is in agreement with the one obtained by magnetoresistance measurements by following the inflection point of the first drop in resistivity, both in pulsed fields (squares) and steady fields (open circles) experiments. The large Nernst signal is indeed a property of the hidden order state.

A finite Nernst signal is expected in a multi-band metal with different types of carriers [41]. Moreover, as illustrated by the case of elemental bismuth [42], the Nernst effect, which tracks the ratio of mobility to the Fermi energy becomes particularly large in a clean semi-metal. In both URu_2Si_2 and $PrFe_4P_{12}$ [43], the large Nernst signal is a property of the ordered state, which can be described as a semi-metal.

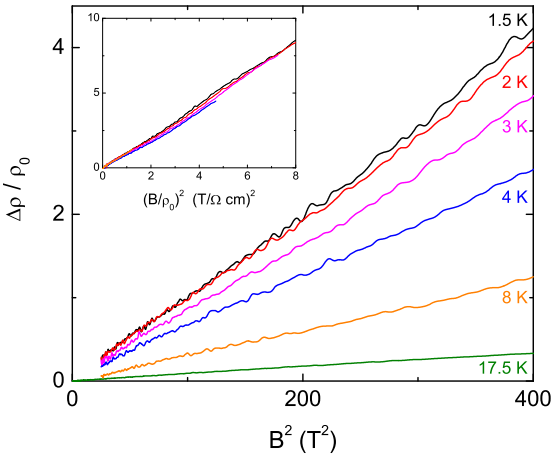

Fig. 3: Magnetoresistance plotted as B^2 for different temperatures. The inset shows a Koehler plot of the magnetoresistance at different temperatures.

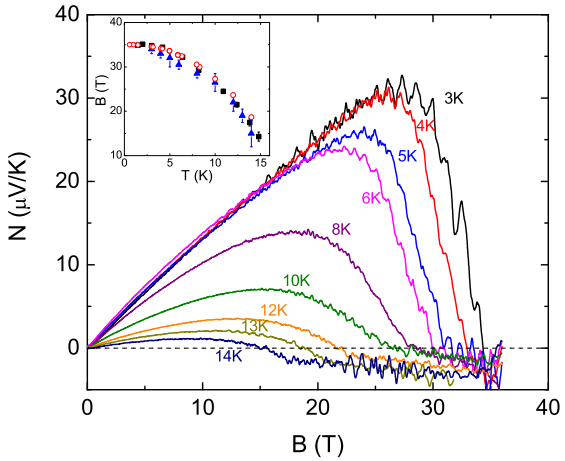

Fig. 4: Magnetic field dependence of the Nernst signal up to 36 T at different temperatures. The curves have been smooth in order to reduce the noise induced by mechanical vibrations seen at high fields. The inset compares the phase diagram (T,B) of URu_2Si_2 in the hidden order obtained from the present MR (square) and Nernst effect (triangles) studies with steady field measurements of the MR (open circles from [29,30]).

Phase II (35 T < B < 37 T). Little is known about phase II, besides that the carrier density is large. Indeed the Hall number is about 20 times lower than in the hidden order state suggesting a large Fermi surface. The reconstruction of the Fermi surface between phase I and II is accompanied by a sharp drop in the mobility in the latter. The small magnitude of the Nernst signal in this phase is, therefore no surprise. Since both this phase and phase IV are high-density metals, an open question is the distinction between these two states. An appealing possibility is that a wave vector different from Q_0 (maybe Q_1) could be a new wave vector leading to less severe Fermi surface reconstruction.

Phase III (37 T < B < 39 T). At 37 T another Fermi surface reconstruction occurs. The Hall number in phase III is rather large but four times lower than in the hidden order state. It has a rather high resistivity which does not vary much with field. All this suggest that it is not simply the reentrant hidden order state. Moreover, since this phase persists in $U(Ru_{0.96}Rh_{0.04})_2Si_2$ where the hidden order phase collapse [30], its presence appears to be insensitive to the physical condition necessary for the emergence of the hidden order. Field induced AF quadrupolar ordered phase may occur, as observed for example in $PrOs_4Sb_{12}$. [44].

Phase IV(B > 39T). The cascade of transitions ends in a final metamagnetic transition at B_M=39 T associated with a magnetization jump of $0.3\mu_B$ [35], leading to a PPM at high fields. In contrast with the hidden-order state, we will see later that the PPM state is a metal with a much larger Fermi surface and much lower mobility.

To sum up, phase I is a semi-metal which a) is compensated, b) is a low carrier-density system, and c) has a rather high electronic mobility. The cascade of phase transitions which take place between 35 T and 39 T, induces several Fermi surface reconstructions. Among all this complexity, URu_2Si_2 shares at least one similarity with other heavy fermions compounds, namely a polarized paramagnetic state reached above 39 T.

Field-induced destruction of electronic correlations. – Fig. 5 compares the temperature dependence of resistivity in the PPM state with the one in the HO, which are not so different. In particular, as seen in the inset of Fig. 5, both present a comparable resistivity below 10 K. However, in spite of their superficial similarity, these two are quite different metals. In the PPM state, the Hall coefficient is small, R_H=0.47×10^{-9}m^3/C, yielding a carrier density of 1.1 hole per U atom. Therefore, a residual resistivity of ρ_{xx} ≈4.4 $\mu\Omega$ *cm* implies a mobility of $\mu \simeq 0.01$ T^{-1}, which is one order of magnitude smaller than the mobility found in the hidden order state.

Let us turn our attention to the magnitude of the inelastic resistivity and its field dependence. Fig. 6(a) and 6(b) show a comparison of the temperature dependence of the transverse MR (plotted versus T^2) for different magnetic fields, in the hidden order state and in the PPM state, respectively. Due to the strong MR at low temperature and to the anomalies of the MR around B_{HO}, it is not possible to reliably extract the A coefficient between 7 T and 40 T. As seen in the inset of Fig. 6(a), at 54 T, the A coefficient attains a magnitude comparable to its zero-field value ($\sim$ 0.15 $\mu\Omega$cmK^{-2}). Using γ=0.06 JK^{-2}mol^{-1}, the Kadowaki-Woods (KW) ratio A/γ^2 at zero field can be estimated to be 40 $\mu\Omega$cmJ^{-2}mol^{2}K^2, four times larger than the universal value introduced by Kadowaki and Woods [45]. According to available theoretical treatments [46,47], the KW ratio is expected to be enhanced when the carrier density decreases, a feature which has been experimentally checked in other heavy-fermion semi-metals such as

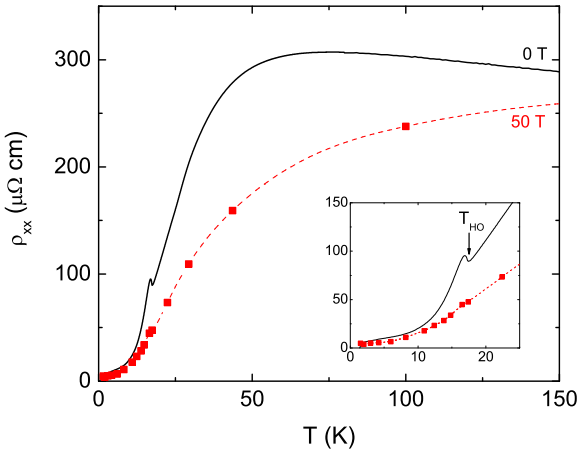

Fig. 5: Temperature dependence of the resistivity of URu_2Si_2 in zero magnetic field and at B=50 T (red squares). The inset shows a zoom at low temperature

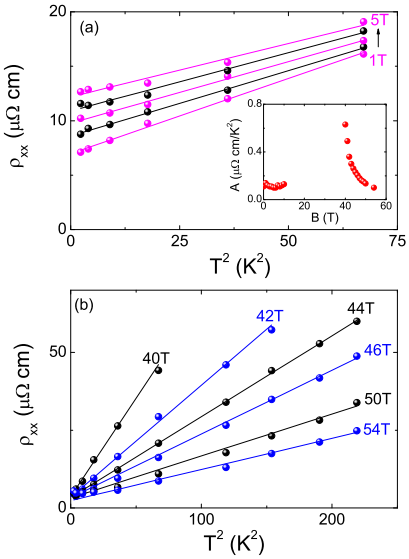

Fig. 6: ρ_{xx} plotted versus T^2 at different magnetic fields (a) in the hidden order state, (b) in the PPM state. The solid lines represent the fits to $\rho_0 + AT^2$ (see text). Inset: Magnetic field dependence of the inelastic term A of the resistivity.

$PrFe_4P_{12}$ [48]. Therefore, the moderately enhanced KW ratio of the hidden order is in qualitative agreement with its reduced carrier density.

Regarding the high-field PPM state, in absence of specific heat and/or dHvA data, the effective mass cannot be quantitatively determined. Given its conventionally large carrier density, it is natural to assume that the KW ratio is not enhanced in the PPM state. Thus, the magnitude of A implies $\gamma \simeq 0.1\ JK^{-2}mol^{-1}$ at B_M. Obviously, the first order nature of the metamagnetic transition in URu_2Si_2 does not wipe out the observation of strong electronic fluctuations above $B = B_M$. In agreement with this observation, Harrison *et al.* have suggested the presence of a putative quantum critical point at $B = B_M$ in URu_2Si_2 [33]. If the long range ordering will collapse, such phenomena suggest the presence of a metamagnetic critical point B_M^* in the temperature-pressure-magnetic field phase diagram. When the ordering (either the hidden order or AF) is destabilized by an external parameter (pressure and/or magnetic field), B_M will not collapse but ends up at a finite critical field value, at it has been identified in the $CeRu_2Si_2$ famillly [49]. Another analogy between URu_2Si_2 and $CeRu_2Si_2$ si the field dependence of the inelastic term of the resistivity (see Fig 7), which appears to show a critical behavior near B_M. However, for $CeRu_2Si_2$ even at $P = 0$, B_M is a sharp crossover field between a low field state dominated by AF fluctuations and a high field regime governed by local fluctuations [50]. By contrast to URu_2Si_2, the number of carrier estimated from Hall measurements does not change significantly through B_M in $CeRu_2Si_2$ [51, 52]. A modification of the FS is clearly detected at B_M and scenarios based on the localization of the $4f$ cerium electrons versus a progressive evolution of the Fermi surface where the heaviest sheet of the polarized Fermi surface becomes completely filled and drops out of transport and thermodynamic properties are still under discussion [49, 53]. Let us remark that in the PPM phase of URu_2Si_2 the derived large number of light carriers near 1 hole per U atom is quite comparable to the value of holes (O.5 hole per U atom) found in band structure calculations in $ThRu_2Si_2$ [22]. It corresponds to the limit of very strong magnetic field where the U atoms are fully polarized and decoupled from the light itinerant band, analogous to that of $ThRu_2Si_2$.

In URu_2Si_2, the new ingredient is the interplay between the ordered phases and Fermi surface reconstruction. Without this reconstruction, the ground state of URu_2Si_2 would be a non-ordered Kondo lattice with an intermediate valent character of the uranium atoms, since the internal structure of the $5f$ angular momentum is wiped out by the large damping of the conduction electrons [13, 37, 54]. URu_2Si_2 would therefore be a paramagnetic mixed valence compound presenting a broad maxima of $C/T \simeq 300$ mJK^{-2}mol^{-1} at about $T \simeq 30$ K and of the susceptibility at $T \simeq 50$ K [37]. These maxima are precursor of metamagnetic phenomena. Below, T_0, the interplay between band structure and multi-ordering leads to drastic change of spin dynamics. The decrease of the carrier density reveals the local properties of the uranium atoms, which is required for the establishment of multiple ordering. At B_M, when the large number of carrier is recovered, C/T reach a value comparable to the maximum value in zero field above T_0. The open question is the description of the uranium atoms in the ordered and paramagnetic phases in terms of localization and itineracy of the two 5f electrons (assuming that the uranium atom is in the U^{4+} configuration). It is worthwhile to compare the (B, T) phase diagram of URu_2Si_2 and the one of some mixed valence systems, such as $YbInCu_4$ [55] or doped Ce metal [56], where an elliptic shape of the boundary

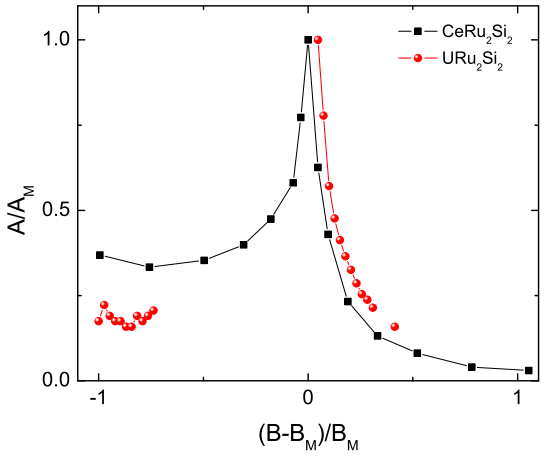

Fig. 7: Comparison of the magnetic field dependence of the inelastic term of the resistivity, A, for URu_2Si_2 and $CeRu_2Si_2$. B_M is the field which corresponds to the metamagnetic transition.

has also been reported. However, when discussing multipole ordering, it should be noted that Yb^{3+} and Ce^{3+} are Kramer's ions and their valence fluctuations involve non-magnetic configuration. In the uranium case, the mixing will involve two possible magnetic configurations: U^{3+} and U^{4+}. Moreover, fancy effects may occur due to crystal field in addition to the transition at T_0, suspected to be non isostructural.

CONCLUSION. – We have discussed the high field transport properties of URu_2Si_2. The hidden order state can be described as a semi-metal which is compensated, has a low carrier-density and has a rather high electronic mobility. This naturally explains the emergence of a large Nernst effect in this phase. Above the destabilization of the hidden order state by a magnetic field of 35 T, a cascade of phase transition occurs and corresponds to several Fermi surface reconstruction, whose origin must be associated with different wave vectors. Above 39 T, a polarized paramagnetic metal is recovered with a high density of carrier and and low electronic mobility.

* * *

We thank D. Aoki, W. Knafo, G. Knebel, and G. Rikken for usefull discussions. Part of this work was supported by the French ANR IceNET and EuroMagNET.

REFERENCES

[1] T.T.M. Palstra *et al.*, Phys. Rev. Lett. **55**, 2727 (1985).
[2] W. Schlabitz *et al.*, Z. Phys. B **62**, 171 (1986)
[3] M.B. Maple *et al.*, Phys. Rev. Lett. **56**, 185 (1986).
[4] P. Santini and G. Amoretti, Phys. Rev. Lett. **73**, 1027 (1994).
[5] A. Kiss and P. Fazekas, Phys. Rev. B **71**, 054415 (2005).
[6] H. Ikeda and Y. Ohashi, Phys. Rev. Lett. **81**, 3723 (1998).
[7] V.P. Mineev and M.E. Zhitomirsky, Phys. Rev. B **72**, 014432 (2005).
[8] P. Chandra *et al.*, Nature (London) **417**, 831 (2002).
[9] C.M. Varma and L Zhu, Phys. Rev. Lett. **96**, 036405 (2006).
[10] C. Broholm *et al.*, Phys. Rev. Lett. **58**, 1467 (1987).
[11] H. Amitsuka *et al.*, J. Magn. Magn. Matter **310**, 214 (2007).
[12] E. Hassinger *et al.*, Phys. Rev. B **77**, 115117 (2008).
[13] A. Villaume *et al.*, Phys. Rev. B **78**, 012504 (2008).
[14] J. Schoenes *et al.*, Phys. Rev. B **35**, 5375 (1987).
[15] K. Behnia *et al.*, Phys. Rev. Lett. **94**, 156405 (2005).
[16] P. A. Sharma *et al.*, Phys. Rev. Lett. **97**, 156401 (2006).
[17] C. Bergemann *et al.*, Physica B **230-232** 348 (1997).
[18] N. Keller *et al.*, J. Magn. Magn. Mater. **177-181** 298 (1998).
[19] H. Ohkuni *et al.*, Philos. Mag. B **79**, 1045 (1999).
[20] Y. Kasahara *et al.*, Phys. Rev. Lett. **99**, 116402 (2007).
[21] C.R. Wiebe *et al.*, Nature Physics **3**, 96 (2007).
[22] H. Harima, private communication.
[23] G. Motoyama *et al.*, Phys. Rev. Lett. **90**, 166402 (2003).
[24] S. Elgazzar *et al.*., arXiv:0809.2887
[25] A. de Visser, Solid State Commun. **64**, 527 (1987).
[26] N.H. van Dijk *et al.*, Phys. Rev. B **56**, 14493 (1997).
[27] F. Bourdarot *et al.*, Phys. Rev. Lett. **90**, 067203 (2003).
[28] K. Bakker *et al.*, Physica B **186-188** 720 (1993).
[29] K.H. Kim *et al.*, Phys. Rev. Lett. **91**, 256401 (2003).
[30] Y.S. Oh *et al.*, Phys. Rev. Lett. **98**, 016401 (2007).
[31] Y.J. Jo *et al.*, Phys. Rev. Lett. **98**, 166404 (2007).
[32] M. Jaime *et al.*, Phys. Rev. Lett. **89**, 287201 (2002).
[33] N. Harrison *et al.*, Phys. Rev. Lett. **90**, 096402 (2003).
[34] M. Date, Physica B **201**, 1 (1994).
[35] T. Inoue *et al.*, Physica B **294-295**, 271 (2001).
[36] N. Harrison *et al.*, J. Mag. Mag. Mat. **272-276**, 135 (2004).
[37] E. Hassinger *et al.*, J. Phys. Soc. Jpn **77**, suppl. A, 172 (2004).
[38] R. Bel *et al.*, Phys. Rev. B **70**, 220501 (2004).
[39] C. Proust *et al.*, unpublished
[40] A. Suslov *et al.*, Phys. Rev. B **68**, 020406 (2003).
[41] R. Bel *et al.*, Phys. Rev. Lett. **91**, 066602 (2003).
[42] K. Behnia *et al.*, Phys. Rev. Lett. **98**, 076603 (2007).
[43] A. Pourret *et al.*, Phys. Rev. Lett. **96**, 176402 (2006).
[44] R. Shiina *et al.*, J. Phys. Soc. Jpn **73**, 3453 (2004).
[45] K. Kadowaki and S. B. Woods, Solid State Comm. **58**, 507 (1986).
[46] H. Kontani, J. Phys. Soc. Jpn. **73**, 518 (2004).
[47] N. E. Hussey, J. Phys. Soc. Jpn. **74**, 1107 (2005).
[48] A. Pourret *et al.*. J. Phys. Soc. Jpn., **77**, Suppl. A, 102 (2008).
[49] J. Flouquet, *Progress in Low Temperature Physics XV* p139-281 (Editor: W.P. Halperin, Elsevier, 2006).
[50] J. Flouquet *et al.*, Physica B **319**, 251 (2002).
[51] R. Daou *et al.*, Phys. Rev. Lett. **96**, 026401 (2006).
[52] S. Kambe *et al.*, J. Low Temp. Phys. **102**, 477 (1996).
[53] S. V. Kusminskiy *et al.*, Phys. Rev. B **77**, 094419 (2008).
[54] J.A. Janik *et al.*, arXiv: 0806.3137.
[55] Y. H. Matsuda *et al.*, J. Phys. Soc. Jpn **76**, 034702 (2007).
[56] F. Drymiotis *et al.*, J. Phys. Cond. Matter **17**, L77 (2005).